Sub-Projection-Noise Sensitivity in Broadband Atomic Magnetometry

M. Koschorreck,[1,*] M. Napolitano,[1] B. Dubost,[1,2] and M. W. Mitchell[1]

[1]*ICFO-Institut de Ciencies Fotoniques, 08860 Castelldefels (Barcelona), Spain*

[2]*Laboratoire Matériaux et Phénomènes Quantiques, Université Paris Diderot et CNRS, UMR 7162, Bâtiment Condorcet, 75205 Paris Cedex 13, France*

(Received 24 November 2009; published 3 March 2010)

We demonstrate sub-projection-noise sensitivity of a broadband atomic magnetometer using quantum nondemolition spin measurements. A cold, dipole-trapped sample of rubidium atoms provides a long-lived spin system in a nonmagnetic environment, and is probed nondestructively by paramagnetic Faraday rotation. The calibration procedure employs as known reference state, the maximum-entropy or ''thermal'' spin state, and quantitative imaging-based atom counting to identify electronic, quantum, and technical noise in both the probe and spin system. The measurement achieves a sensitivity 1.6 dB (2.8 dB) better than projection-noise (thermal state quantum noise) and will enable squeezing-enhanced broadband magnetometry.

DOI: 10.1103/PhysRevLett.104.093602 PACS numbers: 42.50.Lc, 03.67.Bg, 07.55.Ge, 42.50.Dv

Precision magnetic field measurements can be made by optically detecting the Larmor precession produced in a spin-polarized atomic sample [1]. The technique is ultimately limited by quantum noise, present in both the optical measurement and in the atomic system itself. Recent works using large numbers of atoms and long spin coherence times have demonstrated sub-fT/$\sqrt{\text{Hz}}$ sensitivities for dc [2] and rf [3,4] fields for bandwidths of order 1 kHz, surpassing superconducting sensors (SQUIDS) in sensitivity and approaching quantum noise limits. Potential applications of magnetic sensors range from gravitational-wave detection [5] to magnetoencephalography [6].

Atomic spin readout using optical quantum nondemolition (QND) measurement [7,8] allows magnetometry to surpass the standard quantum limit $\delta B \propto 1/\sqrt{N}$ associated with atomic projection noise [9]. Similarly, optical squeezing can surpass the shot-noise limit in optical measurements [10,11]. The measurement is then constrained by the much weaker Heisenberg limit $\delta B \propto 1/N$. This strategy is particularly well adapted to broadband magnetometry, in which repeated or continuous measurements determine a time-varying field. Each QND measurement both indicates the measured spin variable and (ideally) projects the system onto a spin-squeezed state, increasing the sensitivity of subsequent measurements [9,12,13]. To date, QND probing of spin variables has achieved projection-noise limited precision only for magnetically insensitive ''clock'' transitions [12,13] and weakly magnetic atoms with zero total electronic spin [14]. A significant obstacle has been, up to now, the calibration of the spin noise measurements in a magnetically sensitive system [15].

Optically trapped and laser-cooled atoms serve as a broadband magnetometer with a spin measurement bandwidth >1 MHz, orders of magnitude faster than atomic vapor magnetometers [4]. We demonstrate a spin readout noise of $\text{var}(\hat{F}_z) = (515\ \text{spins})^2$, which is 2.8 dB below the thermal spin noise $N_A F(F+1)/3$ and 1.6 dB below the coherent spin state projection noise $N_A F/2$, for N_A atoms of total spin F. The optical QND readout is shot-noise limited. Recent experiments on atom-tuned squeezed light show a reduction of light noise by 5 dB [10], which would reduce the readout noise further, to 6 dB below thermal spin noise.

We establish the projection-noise level by two techniques: a calibrated measurement of the per-atom optical rotation and an analysis of noise scaling when measuring a reference state. The use of noise reference states, e.g., thermal, vacuum, or coherent states of light, is well established in quantum optics. To extend this to spin systems, we use the maximum-entropy state, also known as the ''thermal'' spin state.

Thermal spin states provide a robust tool to characterize optical QND measurements and have several advantages compared to coherent spin states. For instance, photon scattering leaves their quantum noise properties practically unchanged, they are less prone to systematic errors, e.g., due to imperfect spin polarization, and they are less susceptible to magnetic field perturbations because of rotational symmetry.

The collective spin is measured using paramagnetic Faraday rotation with an off-resonant probe. The ensemble spin $\hat{\mathbf{F}}$ interacts with an optical pulse of duration τ and polarization described by the vector Stokes operator $\hat{\mathbf{S}}$ through the effective Hamiltonian [9] appropriate for the case of large detunings and small optical rotations [16,17]

$$\hat{H} = \hbar \frac{G}{\tau} \hat{S}_z \hat{F}_z. \tag{1}$$

We define $\hat{\mathbf{S}}$ in terms of annihilation (creation) operators for left and right circularly polarized light modes, $\hat{a}_\pm (\hat{a}_\pm^\dagger)$,

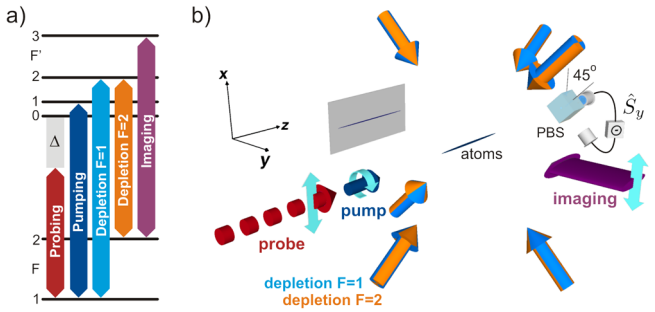

FIG. 1 (color online). (a) Atomic transitions for probing, preparation, and imaging light fields. (b) Atomic ensemble with probing, pumping, and imaging light fields. The polarimeter measures in the 45° basis, i.e., the Stokes component $\hat{S}_y$.

as $\hat{S}_i \equiv (\hat{a}_+^\dagger \hat{a}_-^\dagger)\sigma_i(\hat{a}_+\hat{a}_-)$ [18], where σ_i are the Pauli matrices. The interaction strength G depends on transition dipole moments, optical detuning, and beam and atom cloud geometry [19].

A light pulse experiences a polarization rotation (to first order in $\hat{H}$)

$$\hat{S}_y^{(\mathrm{out})} = \hat{S}_y^{(\mathrm{in})} + G\hat{S}_x^{(\mathrm{in})}\hat{F}_z^{(\mathrm{in})} \tag{2}$$

where the superscripts (in), (out) indicate components before and after the interaction. In a QND measurement of $\hat{F}_z$, the input state has $\langle \hat{S}_x\rangle = N_L/2$ and $\langle \hat{S}_y\rangle = \langle \hat{S}_z\rangle = 0$ such that $\hat{F}_z$ can be estimated as $\hat{F}_z^{(\mathrm{in})} \approx 2\hat{S}_y^{(\mathrm{out})}/GN_L$, where N_L is the number of photons. In addition, macroscopic rotations can be used to measure N_A by polarizing the ensemble such that $\langle \hat{F}_z\rangle = N_A$ prior to probing. We refer to this as "dispersive" atom-number measurement (DANM) and calibrate it using quantitative absorption imaging.

To establish the sensitivity at the quantum level, we note that for input states with $\langle \hat{S}_y^{(\mathrm{in})}\rangle = \langle \hat{F}_z^{(\mathrm{in})}\rangle = 0$, without initial correlation between $\hat{S}_y^{(\mathrm{in})}$ and $\hat{F}_z^{(\mathrm{in})}$, and $\mathrm{var}(\hat{S}_x) \ll \langle \hat{S}_x\rangle^2$, the polarization variance is

$$\mathrm{var}\,(\hat{S}_y^{(\mathrm{out})}) = \mathrm{var}(\hat{S}_y^{(\mathrm{in})}) + G^2\frac{N_L^2}{4}\mathrm{var}(\hat{F}_z^{(\mathrm{in})}). \tag{3}$$

The first term, the input optical polarization, in general has variance $\mathrm{var}(\hat{S}_y^{(\mathrm{in})}) = N_L/4 + \alpha N_L^2$, where the first part is light shot noise and the second technical noise due to variations in the optical state preparation of strength α. Similarly, the second term contributes a variance related to atomic quantum and technical noise, respectively, i.e., $\mathrm{var}(\hat{F}_z) = N_A V_1 + \beta N_A^2 V_1$ where V_1 is the variance per atom and β the amount of technical noise. Finally, we must add a constant "electronic noise" V_E from the detector, and arrive to the measurable signal

$$\mathrm{var}\,(\hat{S}_y^{(\mathrm{meas})}) = V_E + \frac{N_L}{4} + \alpha N_L^2 + G^2 V_1 \frac{N_L^2}{4} N_A + \beta G^2 V_1 \frac{N_L^2}{4} N_A^2. \tag{4}$$

Equation (4) contains the essential elements of the calibration technique. All terms have distinct scaling with photon and atom number, and can thus be separately identified if $\mathrm{var}(\hat{S}_y^{(\mathrm{meas})})$ is measured as a function of N_L and N_A. The terms proportional to N_L and $N_L^2 N_A$ correspond to quantum noise of light and atoms, respectively. Together they provide an absolute calibration of the gain of the detection system and the atom-light coupling G. The remaining terms represent various noise sources. Only if these are simultaneously small relative to the atomic quantum noise, quantum signals will be detectable.

For N_A atoms with spin quantum number F, the reference state is $\rho = \rho_T^{\otimes N_A}$, where ρ_T is the completely mixed state of dimension $2F+1$. In terms of the collective spin $\hat{\mathbf{F}} \equiv \sum_i \hat{\mathbf{f}}^{(i)}$ where $\hat{\mathbf{f}}^{(i)}$ is the spin of the ith atom, the thermal state has zero average value, and a noise of $\mathrm{var}(\hat{F}_n) = \frac{1}{3}F(F+1)N_A$, where $\hat{F}_n$ is any spin component. Hence $V_1 = \frac{1}{3}F(F+1)$.

We now describe in detail the experimental methods. As illustrated in Fig. 1, the experiments are performed with a macroscopic sample of 1×10^6 ^{87}Rb atoms held in an optical dipole trap. After laser cooling, atoms are loaded into the weakly focused beam of a Yb:YAG laser at 1030 nm. Tight (weak) confinement in the transverse (longitudinal) direction produces a sample with high aspect ratio ~240:1. This geometry produces a large atom-light interaction for light propagating along the trap axis. In earlier experiments, we have measured an effective on-resonance optical depth >50 [20].

For each pulse, the photon number N_L is measured by splitting off a portion of the probe beam before it propagates through the atoms, detection with a calibrated photodiode, and numerical integration of the waveform. Absolute measurement of N_A is carried out by quantitative absorption imaging [21]: atoms are transferred into the $F = 2$ hyperfine ground state by a 100 μs pulse of laser light tuned to the $F = 1 \rightarrow F' = 2$ transition. The dipole trap is switched off to avoid spatially dependent light shifts and an image is taken with a 100 μs pulse of linearly polarized light resonant to the $F = 2 \rightarrow F' = 3$ transition. A background image is taken under the same conditions, but without atoms. The observed error in N_A is <4% (rms) including loading fluctuations and measurement noise.

For fast and nondestructive N_A determination, we use DANM: the sample is spin polarized along z by on-axis optical pumping with a 50 μs pulse of circularly polarized light tuned to the $F = 1 \rightarrow F' = 1$ transition. At the same time, light resonant to the $F = 2 \rightarrow F' = 2$ transition (via the MOT beams) prevents accumulation of atoms in $F = 2$. We define a quantization axis by applying a small bias field of ~100 mG along z. Probe pulses with $N_L = 3 \times 10^5$ tuned 800 MHz to the red of the $F = 1 \rightarrow F' = 0$ transition are used to measure the rotation angle $\phi = N_A G_c$. No appreciable atomic depolarization could be observed experimentally after 20 probe pulses, which is supported by calculations that give a destruction of 0.08%

for this number of pulses. The coupling constant $G_c = 6.6(2) \times 10^{-8}$ was calibrated in advance by measuring ϕ for a known N_A, measured by absorption imaging.

Thermal spin states for atoms in the $F = 1$ manifold are produced by repeatedly optically pumping atoms from $F = 1$ to $F = 2$ and back, using lasers tuned to the $F = 1 \rightarrow F' = 2$ and $F = 2 \rightarrow F' = 2$ transitions, and applied via the MOT beams. Each pumping cycle takes 300 μs. To avoid any residual polarization, we apply bias fields of a few hundreds of mG along z, y, and x during the three back-and-forth cycles. Finally, the $F = 2$ manifold is further depleted with a 100 μs pulse of resonant light on the $F = 2 \rightarrow F' = 2$ transition with zero magnetic field. After these steps, no remaining mean polarization along z is observed. This procedure is designed to transfer disorder from the thermalized center-of-mass degrees of freedom to the spin state. Illumination from six directions produces a polarization field with subwavelength structure, in which the atoms are randomly distributed. Possible net imbalances in the pump polarizations are scrambled by the application of different bias fields.

The measurement of $\hat{F}_z$ is made by sending a train of 1 μs long pulses with 10 μs period to the atoms. Each pulse contains 25×10^6 photons, vertically polarized and tuned 800 MHz to the red of the $F = 1 \rightarrow F' = 0$ transition. The output pulses are analyzed in the $\pm 45°$ basis with an ultra-low-noise balanced photodetector [22], giving a direct measure of $\hat{S}_y$. This signal, as well as the signal of the photon-number reference detector, are recorded on a digital storage oscilloscope for later evaluation. While it is possible to vary N_L by adjusting the probe power or pulse duration, it is more convenient to sum the signals from multiple pulses in "metapulses," containing a larger total number of photons. As we are in the linear regime, a metapulse will have the same information as a single higher-energy pulse.

The spin noise measurement proceeds as follows: the dipole trap is loaded (3s) and we wait 400 ms to allow motional thermalization and the escape of untrapped atoms. We then repeat the following sequence 20 times: preparation of a thermal spin state, QND measurement of $\hat{F}_z$, and DANM. In each cycle $\approx 15\%$ of the atoms are lost from the dipole trap, mostly during state preparation, so that different values of N_A are sampled during the measurement sequence. The entire sequence is repeated 500 times to acquire statistics.

Experimental data for atom numbers between 4×10^4 and 8×10^5 and photon numbers up to 10^9 are shown in Fig. 2. The data are fitted with the theoretical expression (4) which is shown as a surface. The deduced coupling constant is $G = 6.65(3) \times 10^{-8}$ and the electronic noise level is $V_E = 4.9 \times 10^5$. The coefficients for the technical noise are $\alpha = 4.3(1) \times 10^{-11}$ and $\beta = 3.1(7) \times 10^{-7}$. Atomic quantum noise dominates above other technical and quantum noise sources for a large range of N_L and N_A, as seen in the vertical panels of Fig. 2.

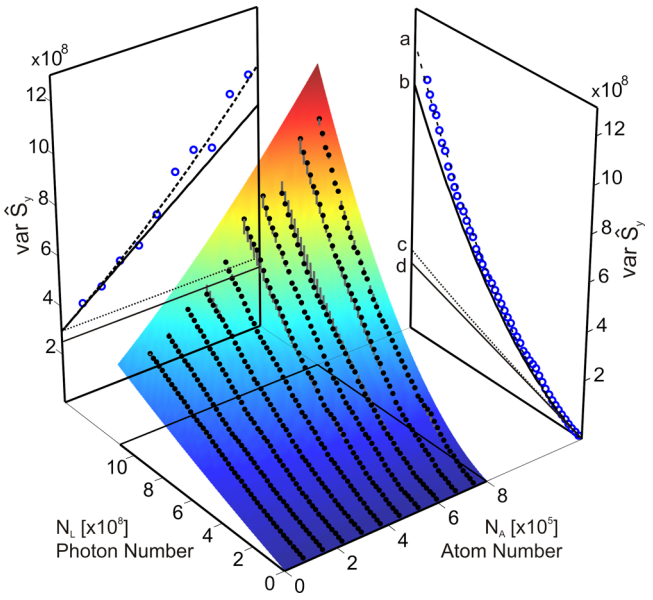

FIG. 2 (color online). Measured variance of $\hat{S}_y$ plotted as black dots and a fit to the data using Eq. (4) as colored surface. The left plot shows the atom-number scaling for $N_L = 10^9$. See Fig. 3 for more details. The right plot shows the photon-number scaling for $N_A = 7.6 \times 10^5$. In the left and right plot curves indicate (from top to bottom): (a) total noise, (b) quantum spin noise plus light noise, (c) light shot and technical noise, and (d) light shot noise.

For the maximum number of photons $N_L = 1 \times 10^9$, the noise scaling with atom number is highlighted in Fig. 3. For the largest atom number measured, i.e., $N_A = 7.6 \times 10^5$, the light shot noise, atomic technical noise, light technical noise, and electronic noise are, respectively, 3.5, 6.3, 11.2, and 30 dB below the quantum noise level of the thermal reference state. The sensitivity of the QND measurement

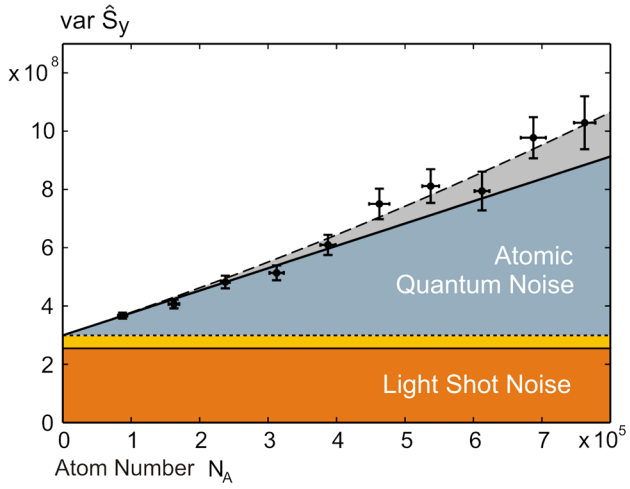

FIG. 3 (color online). Measured variance of $\hat{S}_y$ with statistical errors for $N_L = 10^9$ as a function of atom number. Dashed curve: theoretical curve including technical noise sources. Solid line: pure spin quantum noise. Dotted line: shot noise and technical light noise. Thin solid line: light shot noise. The electronic noise is not plotted because it is negligible for this number of photons.

can be characterized as spin readout noise which is the ratio of the total light noise to atomic quantum noise. From Fig. 3 we can read a spin readout noise which is 2.8 dB (1.6 dB) better than the spin noise for the thermal spin state (coherent spin state, which defines the projection-noise level) at $N_A = 7.6 \times 10^5$ with spin $F = 1$.

The atomic technical noise, shown as the gray area above the thick solid line in Fig. 3, is due to residual spin polarization after the thermal state preparation. The residual spin polarization can be estimated from β and the relative atom-number fluctuations, which are $\simeq 3\%$ (cf. Fig. 3). We find that the maximum fraction of atoms which are not in the completely mixed state is $\sqrt{\beta}/0.03 \simeq 2\%$. From this we can deduce that the systematic error for G is less than 1%. Thus, we conclude the thermal reference state can be well produced and results in a precise calibration of the atom-light interaction strength G. We confirm this measurement with the calibration measurement for the DANM , where we found G_c. This is well suited to measure the atom number N_A quickly and nondestructively, but could lead to an underestimation of the exact value of G_c in the case of imperfect state polarization. Comparing the value from quantum noise scaling G and the calibration value G_c we find an optical pumping efficiency G_c/G of 99(3)% for the polarized state.

The light technical noise may be due to small imbalance of the polarization analyzer and thermal birefringence produced by the dipole laser. Active stabilization of the balancing could improve and reduce the light technical noise considerably. Atomic technical noise may come from classical fluctuations in the lasers during optical pumping.

Extrapolating the technical noise of atoms and light, both remain below their respective quantum noise terms up to $N_{A,\mathrm{qn}} \equiv \beta^{-1} = 3.2 \times 10^6$ and $N_{L,\mathrm{qn}} \equiv (4\alpha)^{-1} = 5.8 \times 10^9$, respectively. It would thus be possible to increase the number of atoms in the trap while remaining projection-noise limited.

In summary, we have demonstrated sub-projection-noise sensitivity of QND spin measurements in a broadband atomic magnetometer. Unlike previous attempts, we use noise scaling and a thermal spin state to obtain an absolute quantification of the measurement noise. The results are confirmed by independent measurement of the atom-light interaction strength. The new method detects different noise sources, i.e., atomic and light quantum and technical noise, and the electronic noise floor, by their respective scaling with atom and photon number. Once reliably characterized with a thermal state, MHz-bandwidth magnetometers applying highly sensitive coherent spin states can be improved beyond the standard quantum limit by applying measurement induced squeezing [23]. Our high-bandwidth system avoids decoherence effects through rapid probing. Similar techniques could also be used with long coherence-time magnetometers [1]. This can have important implications for spatially resolved magnetometry, where cold atomic systems have demonstrated μm resolution [24]. Also in the field of quantum information processing, projection-noise limited QND measurements play an essential role for quantum memory and quantum cloning tasks [25].

We thank Robert Sewell for careful reading of the manuscript. This work was funded by the Spanish Ministry of Science and Innovation under the ILUMA project (Ref. FIS2008-01051) and the Consolider-Ingenio 2010 Project "QOIT."

*marco.koschorreck@icfo.es

[1] D. Budker and M. Romalis, Nature Phys. **3**, 227 (2007).
[2] I. Kominis *et al.*, Nature (London) **422**, 596 (2003).
[3] W. Wasilewski *et al.*, arXiv:0907.2453v3.
[4] V. Shah, G. Vasilakis, and M. V. Romalis, Phys. Rev. Lett. **104**, 013601 (2010).
[5] G. M. Harry *et al.*, Appl. Phys. Lett. **76**, 1446 (2000).
[6] M. Hämäläinen *et al.*, Rev. Mod. Phys. **65**, 413 (1993).
[7] V. B. Braginsky and Yu. I. Vorontsov, Usp. Fiz. Nauk **114**, 41 (1974) [Sov. Phys. Usp. **17**, 644 (1975)].
[8] P. Grangier, J. Courty, and S. Reynaud, Opt. Commun. **89**, 99 (1992).
[9] A. Kuzmich, N. Bigelow, and L. Mandel, Europhys. Lett. **42**, 481 (1998).
[10] G. Hétet *et al.*, J. Phys. B **40**, 221 (2007).
[11] A. Predojevic *et al.*, Phys. Rev. A **78**, 063820 (2008).
[12] Appel *et al.*, Proc. Natl. Acad. Sci. U.S.A. **106**, 10 960 (2009).
[13] M. H. Schleier-Smith, I. D. Leroux, and V. Vuletic, Phys. Rev. Lett. **104**, 073604 (2010).
[14] T. Takano *et al.*, Phys. Rev. Lett. **102**, 033601 (2009).
[15] J. M. Geremia, J. K. Stockton, and H. Mabuchi, Science **304**, 270 (2004); Phys. Rev. Lett. **94**, 203002 (2005); Phys. Rev. Lett. **101**, 039902(E) (2008).
[16] Y. Takahashi *et al.*, Phys. Rev. A **60**, 4974 (1999).
[17] M. Koschorreck and M. W. Mitchell, J. Phys. B **42**, 195502 (2009).
[18] J. Jauch and F. Rohrlich, *The Theory of Photons and Electrons* (Springer, Berlin, 1976).
[19] J. M. Geremia, J. K. Stockton, and H. Mabuchi, Phys. Rev. A **73**, 042112 (2006).
[20] M. Kubasik *et al.*, Phys. Rev. A **79**, 043815 (2009).
[21] H. Lewandowski *et al.*, J. Low Temp. Phys. **132**, 309 (2003).
[22] P. J. Windpassinger *et al.*, Meas. Sci. Technol. **20**, 055301 (2009).
[23] A. André, A. S. Sørensen, and M. D. Lukin, Phys. Rev. Lett. **92**, 230801 (2004).
[24] S. Aigner *et al.*, Science **319**, 1226 (2008).
[25] S. R. de Echaniz *et al.*, Phys. Rev. A **77**, 032316 (2008).